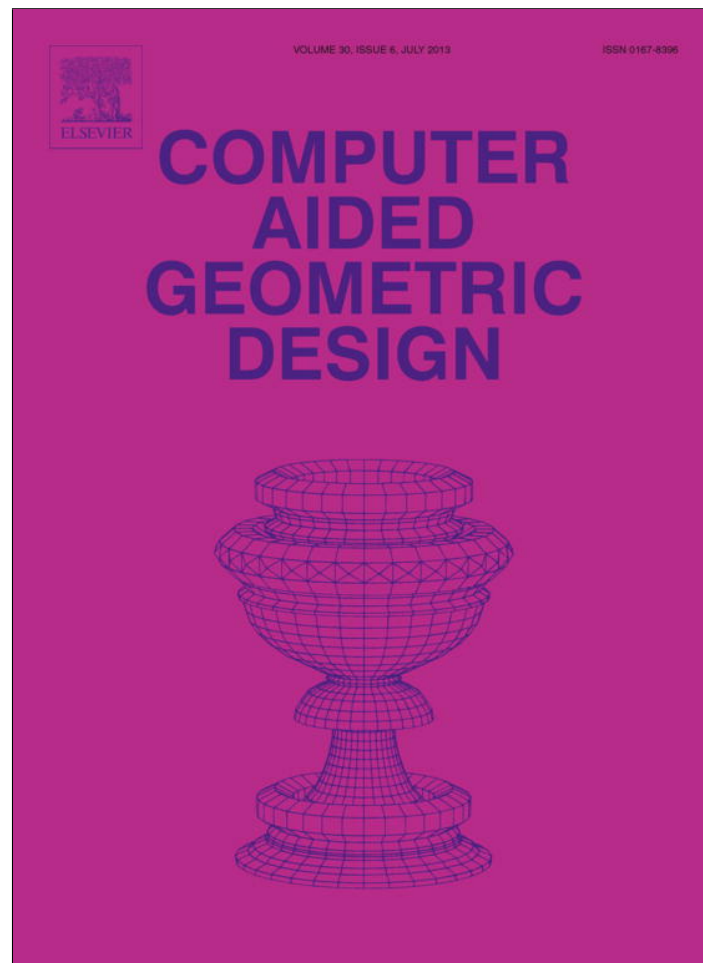


Provided for non-commercial research and education use.
Not for reproduction, distribution or commercial use.



This article appeared in a journal published by Elsevier. The attached copy is furnished to the author for internal non-commercial research and education use, including for instruction at the authors institution and sharing with colleagues.

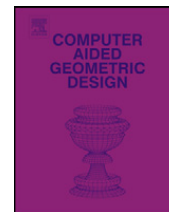
Other uses, including reproduction and distribution, or selling or licensing copies, or posting to personal, institutional or third party websites are prohibited.

In most cases authors are permitted to post their version of the article (e.g. in Word or Tex form) to their personal website or institutional repository. Authors requiring further information regarding Elsevier's archiving and manuscript policies are encouraged to visit:

<http://www.elsevier.com/authorsrights>

Contents lists available at [SciVerse ScienceDirect](http://SciVerse.ScienceDirect.com)

Computer Aided Geometric Design

www.elsevier.com/locate/cagd

Accurate analysis of angiograms based on 3D vector field topology

Thomas Wischgoll

Wright State University, 3640 Col. Glenn Hwy., Dayton, OH 45435, United States

ARTICLE INFO

Article history:

Available online 4 April 2012

Keywords:

3D curve-skeleton
Vector field topology
Sub-voxel precision

ABSTRACT

Cardiovascular diseases are still the number one killer in the United States. The typical diagnostic method is using angiograms for detecting these types of diseases. As is the case with many diseases, early detection can help reduce further progression or enable physicians to take counter measures early on. Hence, accurate analysis techniques are needed for processing these angiogram data sets. In order to perform such analysis of CTA (Computed Tomography Angiograms) data sets, accurate measurements of the coronary vasculature have to be extracted from the volumetric data, such as vessel length, vessel bifurcation angles, cross-sectional area, and vessel volume. These measurements can then be used to discriminate healthy cases from diseased cases. Therefore, this article describes an improved segmentation algorithm based on a hybrid approach between iso-value and image-gradient segmentation and a center line extraction method utilizing 3D vector field topology analysis. Based on the center lines of the coronary vessels found in the angiogram, the quantitative measurements are then computed that can help in the diagnostic process.

© 2012 Elsevier B.V. All rights reserved.

1. Introduction

In order to help in the diagnostic process, extracting morphometric measurements from a specific patient's Computed Tomography Angiogram (CTA) can be very useful in order to tackle life-threatening diseases, such as coronary heart diseases. As a starting point for the extraction of these measurements, a simplified geometric description of the coronary vasculature can be used, such as a curve-skeleton. Curve-skeletons portray the very basic features of an object by describing a thinned version of the object represented as some type of stick model. Accurate curve-skeleton methods can be used for extracting quantitative measurements from computed tomography (CT) scanned vascular structures. Here, the curve-skeleton describes the center lines of the vessels. These can then be used for measuring vessel radius, vessel lengths, and angles between vessels within the volumetric image retrieved by using a CT scanner.

To derive such measurements from the volumetric image, an accurate extraction method for curve-skeletons is desirable. For example, thinning-based techniques that work in the voxel space of the volumetric image tend to generate jagged lines which are in no way suitable for determining angles between vessels. Similarly, inaccuracies can occur when computing the radii of the vessels. Hence, an approach that only uses the volumetric image in order to identify the boundary surface of the contained object is more promising.

The algorithm described in this paper is exactly of this type. It is capable of extracting the boundary surface of an object that is defined by a volumetric image at sub-voxel level. This is obviously a crucial step. Typically, CTA images are somewhat noisy with rather low contrast despite the use of a contrast agent. As the contrast agent is injected into the patient's venous system, it reaches the ventricles first and is then pumped through the coronary vessels and the entire body. As a result,

E-mail address: thomas.wischgoll@wright.edu.

the contrast agent will accumulate not only in the coronary vessels, which the algorithm is supposed to extract, but also the ventricles. Even though most of the smaller vessels supporting the myocardium are too small to show up in the CTA due to the limited resolution of the CT scanner, the contrast agent present in the blood inside those vessels make the myocardium appear brighter. As a result, the contrast between the coronary arteries and the surrounding tissue can be very low making the segmentation step rather challenging.

To segment the boundary of the vasculature accurately, the algorithm described in this paper uses a hybrid approach between iso-value-based boundary extraction and maximal-gradient segmentation to achieve a more accurate identification of the vessel boundary. It then uses the gradient to define a vector field by computing a tetrahedrization of the segmented points. Since there is a gradient vector associated with every segmented point, a vector field can be derived by linearly interpolating within each tetrahedron. A topological analysis of this vector field within the tetrahedra then yields points on the curve-skeleton. By following the topology of the tetrahedrization, points on the curve-skeleton within neighboring tetrahedra can be connected resulting in the entire curve-skeleton.

The next section illustrates related work and compares it to the described approach. Subsequently, the theoretical background with regard to the topological analysis of vector fields is explained. Section 5 shows results of the algorithm applied to various data sets, followed by conclusions and future work.

2. Related work

In order to extract morphometric measurements from the CTA data sets, two initial steps have to be performed: the segmentation of the vessel boundary and the computation of the curve-skeleton. There is a vast variety of different segmentation techniques. Simple thresholding techniques segment the data based on whether the intensity value exceeds a pre-selected threshold. [Sezgin and Sankur \(2004\)](#) provide an overview over such techniques including a quantitative performance evaluation. Other approaches are based on region growing ([Tremeau and Borel, 1997](#)). Starting at a seed point, the region propagates depending on a certain homogeneity criterion, typically involving a threshold. A variation of this approach was introduced by [Phole and Toennies \(2001\)](#) who introduced a region growing algorithm that learns its homogeneity criterion automatically from characteristics of the region to be segmented. Other approaches simulate the flooding of water by interpreting intensity values as height values resulting in the computation of watersheds within the data that resemble the area of interest ([Vincent and Soille, 1991](#)). By forming an energy-minimizing spline that is guided by external constraint forces and influenced by image forces that pull it toward features such as lines or edges within the image, an active contour or snake algorithm can be designed ([Kass et al., 1987](#)). Another technique is based on level sets. An interface or front is used that describes a closed, non-intersecting hyper-surface that follows along the gradient field of the data set by solving the Hamilton–Jacobi equation ([Malladi et al., 1995](#)). [Kindlmann et al. \(2009\)](#) utilize a particle system that computes sampling of crease features to segment scanned medical data sets.

For extracting curve-skeletons or medial axis, several different approaches can be found in the literature. A very good overview of available techniques can be found in the paper by [Cornea et al. \(2005\)](#). Some methods start with all voxels of a volumetric image and use a thinning technique to shrink down the object to a single line. Directional thinning approaches use a specific order in which voxels are removed ([Tsao and Fu, 1981](#)). Ideally, the topology of the object should be observed. Such an approach was proposed by [Lobregt et al. \(1980\)](#). The disadvantage of this approach is that it tends to produce jagged lines which do not allow accurate measurements of angles between parts of the object, such as individual vessels of a vascular structure. Other approaches ([Svensson et al., 2002](#)) classify the voxels in different groups, such as edge, inner, curve, or junction and re-classified after removal of a voxel. The disadvantage of thinning algorithms is that they can only be applied to volumetric data sets due to the nature of these algorithms.

Other approaches use the distance transform or distance field in order to obtain a curve-skeleton. For each point inside the object, the smallest distance to the boundary surface is determined. For this, the Euclidean metric or the $\langle 3, 4, 5 \rangle$ metric ([Borgefors, 1996](#)) can be used. Voxels representing the center lines of the object are identified by finding ridges in the distance field. The resulting candidates must then be pruned first. The resulting values are then connected using a path connection or minimum span tree algorithm ([Zhou et al., 1998](#)). Methods used for identifying points on the ridges include distance thinning ([Pudney, 1998](#)), divergence computing ([Bouix and Siddiqi, 2000](#)), gradient searching ([Bitter et al., 2001](#)), thresholding the bisector angle ([Malandain and Fernandez-Vidal, 1998](#)), geodesic front propagation ([Perchet et al., 2004](#)), or shrinking the surface along the gradient of the distance field ([Schirmacher et al., 1998](#)). The distance field can also be combined with a distance-from-source field to compute a skeleton ([Zhou and Toga, 1999](#)).

Techniques based on Voronoi diagrams ([Amenta et al., 2001](#); [Dey and Goswami, 2003](#)) define a medial axis using the Voronoi points. Since this approach usually does not result in a single line but rather a surface shaped object, the points need to be clustered and connected in order to obtain a curve-skeleton. Voronoi-based methods can be applied to volumetric images as well as point sets. Due to the fact that clustering of the resulting points is required these approaches lack some accuracy. In addition, they tend to create points outside the object itself if there is an open or missing area within the object's boundary.

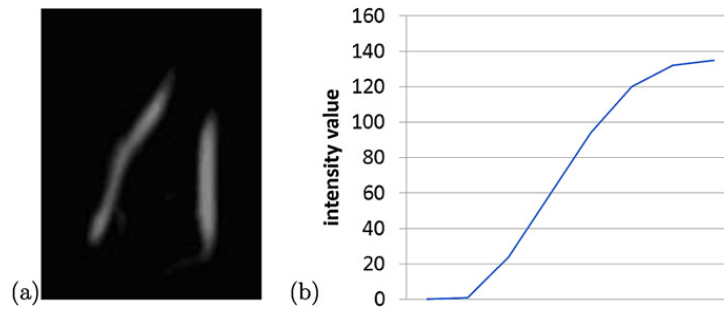


Fig. 1. Sample sub-section of a slice of a typical CT scanned data set illustrating the different intensities of vessels depending on their size and the fading of the intensity due to the point spread function (a) and the increase in intensity at the vessel boundary for one transition within that same image (b).

3. Background

Before illustrating the algorithm used to extract quantitative information from the CT scanned volumetric images, the theoretical foundation of the methodology will be outlined.

The algorithm described in this paper uses the topology of a vector field defined based on a linear interpolation within tetrahedra. Thus, the vector field is defined by four vectors located at the vertices of a tetrahedron. The vector field inside a tetrahedron is interpolated linearly by computing the barycentric coordinates of the point within the tetrahedron. These coordinates are then used as weights for linearly combining the four vectors defined at the vertices of the tetrahedron to compute the interpolated vector. The advantage of such a linear interpolation is an easier classification of topological features, mainly critical points, which is briefly outlined in the following.

Critical points, also known as singularities, are an important feature from a topological point of view since they are used as starting points for the topological analysis. For vector fields described on tetrahedral grids, the vector field inside each cell can be approximated by linear interpolation and topological features extracted based on the eigenvalues and eigenvectors of the interpolating matrix (Hirsch and Smale, 1974). Assuming the non-trivial case where the vector field is not entirely zero, there cannot be more than one singularity, i.e. location where the vector field assumes a value of zero, located within one tetrahedron when using linear interpolation. Negative eigenvalues describe an attracting feature in the corresponding eigenvalue direction, whereas positive eigenvalues result in a repelling feature. This allows for a classification of the singularity based on the eigenvalues. For example, a singularity with all negative eigenvalues is considered a sink.

In order to identify a center line, singularities with an attracting feature within two dimensions are of interest. These types of singularities are attracting node and focus singularities (two eigenvalues are negative), as well as attracting spiral singularities (two eigenvalues have a non-zero imaginary part). For example, if a spiraling effect within a cell of the vector field is present in two of the three dimensions as described by the two negative eigenvalues, then the eigenvector corresponding to the remaining eigenvalue defines the rotational axis of this vector field. This rotational axis then corresponds to a segment of the center line that the algorithm is trying to find.

4. Methodology

Extracting quantitative measurements from volumetric data involves several steps. First, the boundary of the coronary vessels needs to be segmented. Then, a vector field is computed that is orthogonal to the object's boundary surface. Once the vector field is computed, the center lines of the vessels can be determined by applying a topological analysis to this vector field. In a last step, measurements are computed based on the center line and the boundary of the vessels. The following subsections explain these steps in detail.

4.1. Extracting the boundary of the object

When segmenting objects within CT scanned volumetric data sets, there are typically two different artifacts one has to deal with: partial volume effects (Meltzer et al., 1990) and the point spread function. The former stems from the fact that the object's boundary typically does not fall directly on a specific voxel but instead is located somewhere in between a set of voxels. To account for this effect, extracting the object's boundary in an accurate fashion requires the identification of said boundary at a sub-voxel level. The point spread function on the other hand describes the extent of a specific voxel that bleeds into neighboring voxels. If we were to scan an object of just one voxel in diameter which falls exactly onto a scanned voxel, we would see some fading into the surrounding area. The amount of spreading can vary depending on the scanner and its settings.

As a result of the point spread function, the boundary of the vessel is not a sharp jump in intensity, but a gradual increase instead. Fig. 1(a) shows an example of a couple of vessels from one of the slices of a CTA data set. Part (b) of that same figure shows the gradual transition from the outside area (intensity value 0) to the center of the vessel (intensity value 135). In addition, the intensity value of the vessel can vary depending on its size, i.e. larger vessels appear brighter in the scan compared to smaller vessels. One approach often used to segment the vessels is choosing an iso-value for

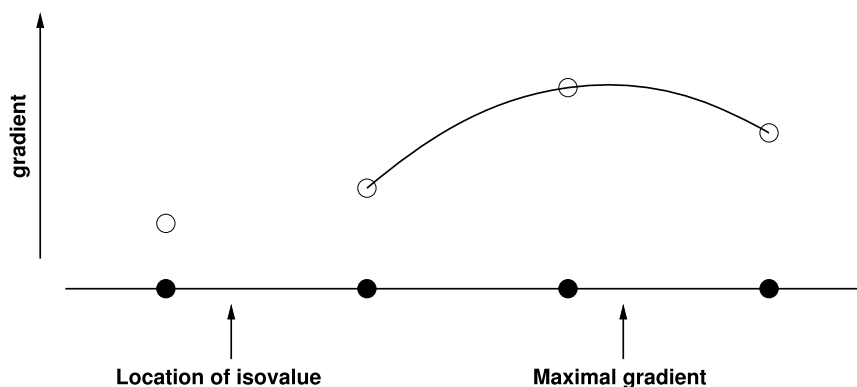


Fig. 2. An example for finding the maximal gradient location where the algorithm detects where the iso-value is assumed and then moves in the direction of increasing image gradients to find the maximal gradient.

the intensity threshold and then computing an iso-surface based on that value. While this approach does result in a sub-voxel segmentation of the vessels, it does not guarantee accuracy. The iso-value has to be chosen in such a way that it is small enough to pick up the smaller vessels that appear at a lower intensity in the volumetric data. Due to the gradual increase in intensity resulting from the point spread function and the fact that the intensity changes depending on the vessel thickness, this then means that there is essentially one size of vessels where the iso-value extracts the boundary accurately. For smaller vessels, the iso-value-based approach underestimates the vessel size, whereas for larger vessels it overestimates it resulting in inaccurate measurements. In the example shown in Fig. 1, any iso-value between 1 and 130 would segment the vessel. However, the diameter of the vessel would seem to increase with a decreasing iso-value.

Better results can be achieved by looking for the maximal gradient in between a set of voxels (Wischgoll, 2008). While this approach segments the vessel boundary very well, it typically picks up on noise within the image very easily as it detects any change in the image gradient above the chosen threshold. This is a big issue especially with CT angiograms. Naturally, the myocardium is perfused with blood and the ventricles are constantly filled with blood as well. As a result the contrast agent used to enhance the vessels also reaches those areas, thereby reducing the contrast of the vessels resulting in a significant amount of noise. On the other hand, an iso-value-based approach does pick up on the vessels nicely as the intensity range for blood is usually consistent among different scans. It just does not segment the boundary accurately enough due to the point spread function. In order to get the advantages of both approaches, a hybrid method was developed.

Similar to the way the Marching Cubes algorithm processes the rectangular grid defined by the voxels making up the volumetric data set, the points in between two voxels connected along an edge of that grid are computed where the iso-value is assumed. The edge is then followed further down to the neighboring voxels, potentially following along a few edges of the volumetric grid, to find the maximal gradient along that direction. The actual location of the maximal gradient in between two voxels is identified based on the three adjacent voxels lined up along a straight edge. Their intensity values can be used to form a quadratic polynomial whose maximal value is determined. The location of that maximum then resembles the location of the maximal gradient and therefore the location of the vessel boundary. Fig. 2 shows an example where the algorithm starts at the location of the iso-value and moves further to the right where the gradient is increasing to find the maximum. The maximal number of voxels that have to be traversed in order to find the maximal gradient depends on the point spread function, or to be more precise on its kernel size. In our implementation, the search radius included the next ten voxels. Once all the maximal gradients are identified using this approach the vessel boundary is segmented. Similar to a pure iso-value-based approach, noisy voxels significantly below the intensity value of blood are skipped. This step then results in the vessel boundary being extracted accurately at a sub-voxel level independent of the actual shape and extent of the point spread function or the size of the vessel.

4.2. Determining the curve-skeleton

In order to determine the curve-skeleton of the object, a tetrahedrization of the all points on the object's boundary is computed first using Si's (2004) very fast implementation of a Delaunay tetrahedrization algorithm. Based on the gradient vectors, which point to the inside of the object, outside tetrahedra can be distinguished from tetrahedra that are located inside the object. This way, all outside tetrahedra can be removed, leaving a Delaunay tetrahedrization of the inside of the object only. Since gradient vectors are known for each vertex of every tetrahedron, a vector field can be defined based on this tetrahedrization by interpolating linearly within each tetrahedron. This vector field is then used for identifying points of the curve-skeleton which are connected with each other later on.

Since the vector field is now defined within the entire object, one could use an approach similar to the one used by Cornea et al. (2005) at this point and compute the 3D topological skeleton of the vector field which yields the curve-skeleton of the object. However, since singularities are very rare in a 3D vector field, Cornea et al. had to introduce additional starting points for the separatrices, such as low divergence points and high curvature points, in order to get a good representation

of the curve-skeleton. Thus, a different approach is described in this paper that analyzes the vector field based on the singularities for each of the tetrahedra.

The previous algorithm for extracting center lines developed by the author (Wischgoll, 2008) was based on the analysis of the 2D vector field on the faces of the tetrahedra. Particularly, that algorithm identified center points by locating 2D singularities within the vector field defined on the faces of the tetrahedra that are orthogonal to the vessel direction. However, this introduces an artificial grid structure defined by the tetrahedrization onto the volumetric data, which is in no relation to that data. In addition it requires the vectors to be somewhat lined up with those faces, i.e. the faces need to be close to the cross-sectional area of the vessels. As a result, the center line may not be fully extracted in some areas leading to gaps that have to be closed in a subsequent step.

To avoid these drawbacks of the 2D-based approach, the new algorithm considers the 3D vector field defined by the vectors associated with the vertices of each tetrahedron defining a linear 3D vector field inside the tetrahedron. As previously described, a topological analysis can be performed on that vector field revealing up to one singularity. This assumes that the vector field is non-trivial, i.e. entirely zero or zero along a single line, in which the algorithm simply identifies that line as part of the center line.

As the linear vector field defined within each tetrahedron is actually not restricted to the tetrahedron, but extends infinitely in all three dimensions, the singularity may not be located inside that tetrahedron. Similar to the previous 2D algorithm, where focus and spiral singularities were identified within the vector field projected onto the faces of the tetrahedra, this algorithm now looks for singularities that have a focus or spiraling property in two out of the three dimensions. Since the vector field is defined in such a way that the vectors are always pointing to the inside of the vessels, the singularity needs to be an attractor. Hence, two of the eigenvalues have to be negative to identify such a singularity. The rotational axis of the spiraling singularity can be identified by the eigenvector associated with the third eigenvalue. This rotational axis is then co-located with a segment of the center line. As a result, the algorithm now has to intersect this rotational axis, defined by the straight line starting at the location of the singularity and the direction of the third eigenvector, with the faces of the tetrahedron to identify the segment of the center line. Obviously, if there is no intersection between the rotational axis and the tetrahedron, this tetrahedron does not contribute to the center lines.

It should be noted that the quality of the resulting center lines is as good as the results of the 2D algorithm. The intersection between the rotational axis of the singularity and a face of a tetrahedron results in the same point as was calculated by the 2D algorithm, assuming the face is approximately cross-sectional to the vessel. This can be easily seen by considering the corresponding vector field. The 2D algorithm would have projected the vectors onto the face. Since the vector field was spiraling around the rotational axis, this projection then removes the directional component of the vectors orthogonal to the face. This then results in a 2D spiral singularity located exactly at the same spot where the rotational axis of the 3D vector field intersects the face. Hence, the center points identified by the 2D algorithm are also identified by the 3D algorithm. However, the major advantage of the 3D approach is that no artificial grid structure is imposed on the data, thereby eliminating the requirement of faces having to be cross-sectional to the vessel. As a result, significantly fewer gaps occur within the center lines as the 3D approach is able to detect more center points, yet the high accuracy of the original algorithm is preserved entirely.

Once the individual segments of the center line are identified, they need to be connected in order to retrieve the entire curve-skeleton. Since the tetrahedrization describes the topology of the vasculature, the connectivity information of the tetrahedra can be used. Thus, identified segments of the center line of neighboring tetrahedra are connected with each other forming the entire curve-skeleton.

4.3. Extracting morphometric measurements

Based on the center line of the vessels and the vessel boundary, morphometric measurements can be extracted for a specific specimen. The length of a vessel can be determined as the sum of the center line segments for that particular vessel. At every vessel bifurcation, where a second vessel forks off of another vessel, the center lines of those vessels form a similar bifurcation. Based on those center lines various bifurcation angles can be identified. The vessel radius can be computed as the distance between the center line and the vessel boundary at any specific location within the vasculature. Similarly, the cross-sectional area is computed as the surface area formed by the vessel boundary surrounding a point on the center line. The volume of a vessel is computed as the volume surrounding the center line limited by the vessel boundary.

The vessel length and vessel volume can then be computed for the so-called crowns of the vasculature. A crown is defined as all vessels downward from a given bifurcation. Hence, when representing the segmented vasculature as a tree according to the extracted center lines, a crown simply corresponds to a sub-tree starting at a bifurcation of that tree. The software described in this paper can then compute the volume of the entire crown and the vessel length as the sum of all vessel lengths within this crown. This can be very helpful for diagnostic purposes as will be shown in the next section.

5. Results

The algorithm was tested on 12 different CTA data sets. Due to the use of the hybrid segmentation algorithm the algorithm is very insensitive to slight changes in the intensity values of the vessels allowing the algorithm to accurately process all scans with the exact same threshold settings yet find the vessel boundary accurately at sub-voxel precision. Due to the

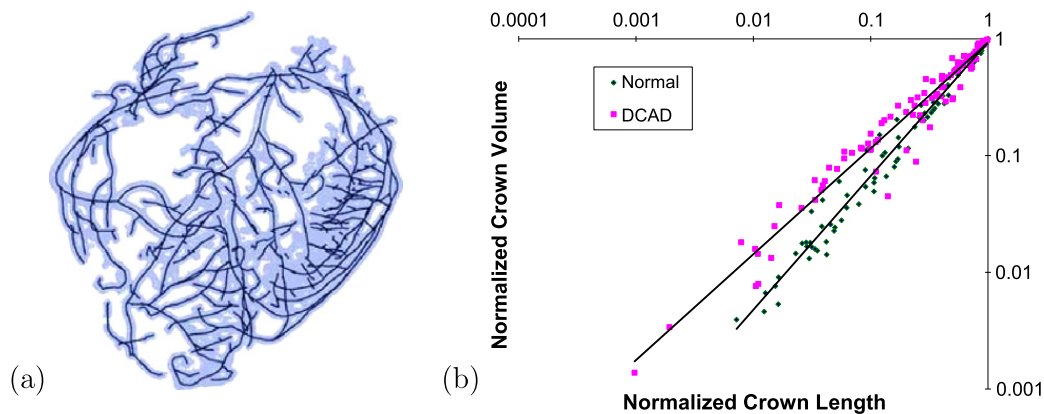


Fig. 3. Centerlines computed by the algorithm based on the segmented boundary of the vascular structure (a) and a comparison of the relation between normalized crown volume and normalized crown length for healthy and diseased cases (b). (For interpretation of the references to color in this figure, the reader is referred to the web version of this article.)

fact that the extracted center points are mainly identical to the ones of the author's previous algorithm (Wischgoll, 2008) as illustrated in the previous section, the high accuracy of the quantitative measurements is preserved. Fig. 3(a) shows sample results for the segmented vessel boundary and the resulting centerlines.

For a scan resolution of 0.6 mm, the root mean square error for the vessel radii measurement is 0.16 mm and the average deviation between the computed measurements and optical measurements remains at 0.13 mm. This corresponds to an accuracy of around a quarter voxel. The major advantage of the algorithm described here over the previous approach is that the method described in this paper no longer imposes an artificial grid structure defined by the tetrahedrization onto the data set, i.e. it is no longer required that there are faces of tetrahedra that are approximately cross-sectional to the vessel. The new method is capable of identifying center points entirely independent of the orientation of the tetrahedra resulting in fewer gaps within the center line and therefore a better extraction of the curve-skeleton of the vasculature. This then allows the algorithm to extract quantitative measurements in form of vessel radius, vessel length, vessel volume, or cross-sectional area at a very high accuracy as described earlier.

Based on the quantitative measurements, the geometric shape of the vasculature can be reconstructed and visualized. Additional information can be added to the visualization in the form of overlays. These overlays can then display vessel volume or surface area for selected vessel segments to further investigate the patient specific data.

The geometric structure of the vasculature typically follows the minimal work principle, i.e. it is designed in such a way that the cost of operation of the organ is minimized while still allowing the organ to fulfill its designated task properly. This minimal work principle applies to both the relation of the vessel diameter of the parent and daughter vessels at each bifurcation and the angles they form (Murray, 1926a) as well as to the volume of the vessels (Murray, 1926b). This then results in scaling laws for the relation between the vessel volume and vessel length describing an exponential relation between those two measurements (Kassab, 2006). This fact allows for a comparison between healthy and diseased patient data sets. Eight out of the twelve data sets that were processed using the algorithm described in this paper were from diseased patients (Metabolic Syndrome), whereas four were from healthy patients. For all crowns extracted from all twelve CTA data sets, the volume of all vessels from those crowns was determined (crown volume) as well as the accumulative vessel lengths (crown length). In order to compare among different patients, the crown volume and crown length was normalized by using the vessel volume and the accumulated vessel length of the entire vasculature as the maximum identified with the value 1. The crown volumes and crown lengths are then divided by those maximal values so that the values now range from zero through one. Fig. 3(b) shows the graphs representing the relation between the normalized crown length and normalized crown volume. Since the scales of the axes are logarithmic, the relation is described by a power law representing the expected exponential relation confirming the scaling law for the vasculature. Interestingly, our preliminary data indicates that there is a difference between healthy (blue) and diseased patient data (pink) resulting in a different exponent for the exponential relation between crown volume and crown length. This means that the diseased state results in a reduction of the volume per length of the vasculature. The change in the exponent, i.e. the reduction in vascular volume, can then be used for diagnostic purposes. The important aspect of this finding is that not only local obstructions within the vasculature, which current techniques can identify, are detected but also changes in the vasculature that stretch over larger areas of the vasculature but restrict the blood flow due to the reduction in vessel volume in the exact same way as local obstructions. This form of heart disease is typically not detected by current diagnostic techniques.

6. Conclusion and future work

In this paper, an algorithm for extracting morphometric measurements from CTA data sets given was presented. The described algorithm is based on a topological analysis of a vector field derived from the configuration of the point set describing the object's boundary contained in the data set to determine the curve-skeleton of the vasculature. Due to

the fact that it is no longer necessary to compute the vector field on a multitude of points but instead only for points on the object's boundary the described algorithm is significantly faster than other vector-field-based approaches while still preserving a high accuracy of the extracted curve-skeleton. For a CTA data set, the algorithm needed a little more than an hour to determine the curve-skeleton and extract the measurements.

The preliminary data confirms the morphometric analysis of the vasculature found in the literature. The diagnostic potential of the extracted measurements is very promising. Further studies need to be performed with a larger data base to confirm the findings. 139 patient CTA data sets were already acquired from 37 healthy and 102 diseased patients, which will be processed in the near future to confirm our findings on a larger scale.

Acknowledgements

The author would like to thank Ghassan Kassab and Jenny Choy-Zorrilla for providing the heart data sets. I would also like to thank the Wright State University and the Ohio Board of Regents for supporting this research as well as Hang Si and Nicu Cornea for making their source code publicly available. This research was supported in part by the National Institute of Health-National Heart, Lung, and Blood Institute Grant HL-092048.

References

- Amenta, N., Choi, S., Kolluri, R.-K., 2001. The power crust. In: Proc. of 6th ACM Symp. on Solid Modeling, pp. 249–260.
- Bitter, I., Kaufman, A.E., Sato, M., 2001. Penalized-distance volumetric skeleton algorithm. *IEEE Transactions on Visualization and Computer Graphics* 7 (3), 195–206.
- Borgefors, G., 1996. On digital distance transforms in three dimensions. *Computer Vision and Image Understanding* 64 (3), 368–376.
- Bouix, S., Siddiqi, K., 2000. Divergence-based medial surfaces. In: ECCV, vol. 1842. Springer-Verlag, pp. 603–618.
- Cornea, N.D., Silver, D., Min, P., 2005. Curve-skeleton applications. In: Proceedings IEEE Visualization, pp. 95–102.
- Cornea, N.D., Silver, D., Yuan, X., Balasubramanian, R., 2005. Computing Hierarchical Curve-Skeletons of 3D Objects. *The Visual Computer (Springer)* 21 (11), 945–955.
- Dey, T.K., Goswami, S., 2003. Tight cocone: a water-tight surface reconstructor. In: Proc. 8th ACM Sympos. Solid Modeling Applications, pp. 127–134; *Journal of Computing and Information Science in Engineering* 30, 302–307.
- Hirsch, M.W., Smale, S., 1974. *Differential Equations, Dynamical Systems and Linear Algebra*. Academic Press.
- Kass, M., Witkin, A., Terzopoulos, D., 1987. Snakes: active contour models. *International Journal of Computer Vision* 1 (4), 312–331.
- Kassab, G.S., 2006. Scaling laws of vascular trees: of form and function. *American Journal of Physiology. Heart and Circulatory Physiology* 290, H894–H903.
- Kindlmann, G.L., Estepar, R.S., Smith, S.M., Westin, C., 2009. Sampling and visualizing creases with scale-space particles. *IEEE Transactions on Visualization and Computer Graphics* 15 (6).
- Lobregt, S., Verbeek, P.W., Groen, F.C.A., 1980. Three-dimensional skeletonization: principle and algorithm. *IEEE Transactions on Pattern Analysis and Machine Intelligence* 2 (1), 75–77.
- Malandain, G., Fernandez-Vidal, S., 1998. Euclidean Skeletons, *Image and Vision Computing* 16, 317–327.
- Malladi, R., Sethian, J.A., Vemuri, B.C., 1995. Shape modeling with front propagation: a level set approach. *IEEE Transactions on Pattern Analysis and Machine Intelligence* 17 (2), 158–175.
- Meltzer, C.C., Leal, J.P., Mayberg, H.S., Wagner, H.J., Frost, J.J., 1990. Correction of PET data for partial-volume effects in human cerebral cortex by MR imaging. *Journal of Computer Assisted Tomography* 14 (4), 561–570.
- Murray, C.D., 1926a. The physiological principle of minimum work applied to the angle of branching of arteries. *The Journal of General Physiology* 9 (6), 835–841.
- Murray, C.D., 1926b. The physiological principle of minimum work. I. The vascular system and the cost of blood volume. *Physiology* 12, 207–214.
- Perchet, D., Fetita, C.I., Preteux, F., 2004. Advanced navigation tools for virtual bronchoscopy, In: Proc. SPIE Conf. on Image Processing: Algorithms and Systems III, vol. 5298.
- Phole, R., Toennies, K.D., 2001. A new approach for model-based adaptive region growing. In: *Medical Image Analysis, Lecture Notes in Computer Science*, vol. 2124, pp. 238–246.
- Pudney, C., 1998. Distance-ordered homotopic thinning: a skeletonization algorithm for 3D digital images. *Computer Vision and Image Understanding* 72 (3), 404–413.
- Schirmacher, H., Zöckler, M., Stalling, D., Hege, H., 1998. Boundary surface shrinking – a continuous approach to 3D center line extraction. In: Proc. of IMDSP, pp. 25–28.
- Sezgin, M., Sankur, B., 2004. Survey over thresholding techniques and quantitative performance evaluation. *Journal of Electronic Imaging* 13 (1), 146–168.
- Si, H., 2004. TetGen, a quality tetrahedral mesh generator and three-dimensional Delaunay triangulator. WIAS technical report No. 9.
- Svensson, S., Nystrom, I., Sanniti di Baja, G., 2002. Curve skeletonization of surface-like objects in 3D images guided by voxel classification. *Pattern Recognition Letters* 23 (12), 1419–1426.
- Tremeau, A., Borel, N., 1997. A region growing and merging algorithm to color segmentation. *Pattern Recognition* 30 (7), 1191–1203.
- Tsao, Y.F., Fu, K.S., 1981. A parallel thinning algorithm for 3D pictures. *Computer Vision, Graphics, and Image Processing* 17, 315–331.
- Vincent, L., Soille, P., 1991. Watersheds in digital spaces: an efficient algorithm based on immersion simulations. *IEEE Transactions on Pattern Analysis and Machine Intelligence* 13 (6), 583–598.
- Wischgoll, Th., 2008. Computing center-lines: an application of vector field topology. In: Hege, H.-C., Polthier, K., Scheuermann, G. (Eds.), *Topology-Based Methods in Visualization II*, pp. 177–190.
- Zhou, Y., Toga, A.W., 1999. Efficient skeletonization of volumetric objects. *IEEE Transactions on Visualization and Computer Graphics* 5 (3), 196–209.
- Zhou, Y., Kaufman, A., Toga, A.W., 1998. Three-dimensional skeleton and centerline generation based on an approximate minimum distance field. *The Visual Computer* 14, 303–314.